JACS
JOURNAL OF THE AMERICAN CHEMICAL SOCIETY
Article
Cite This: J. Am. Chem. Soc. XXXX, XXX, XXX−XXX
pubs.acs.org/JACS

Guest-Dependent Dynamics in a 3D Covalent Organic Framework

Yichong Chen,[‡,†] Zhao-Lin Shi,[‡,§,∥,†] Lei Wei,[‡,†] Beibei Zhou,[‡] Jing Tan,[‡] Hao-Long Zhou,*[,‡] and Yue-Biao Zhang*[,‡,§,∥]

[‡]School of Physical Science and Technology, ShanghaiTech University, Shanghai 201210, China
[§]Joint Laboratory of Low-Carbon Energy Science, Shanghai Advanced Research Institute, Chinese Academy of Sciences, Shanghai 201203, China
[∥]University of Chinese Academy of Sciences, Beijing 100049, China

Supporting Information

ABSTRACT: Guest-dependent dynamics having both crystal contraction and expansion upon inclusion of various guests is uncovered in a 3D covalent organic framework (COF) prepared with a facile and scalable method. A molecular-level understanding of how the framework adjusts the node geometry and molecular configuration to perform significant contraction and large amplitude expansion are resolved through synchrotron in-house powder X-ray diffraction (PXRD) and Rietveld refinements. We found that the COF adopts a contracted phase at ambient conditions upon capturing moisture and is also adaptive upon inclusion of organic solvents, which is highlighted by a large crystal expansion (as large as 50% crystallographic volume increment and a 3-fold channel size enlargement). With this new knowledge of the structural adaptability, the diverse responses and coherent switchability are thereby presented to pave the way to rational design and deliberate control of dynamic COFs.

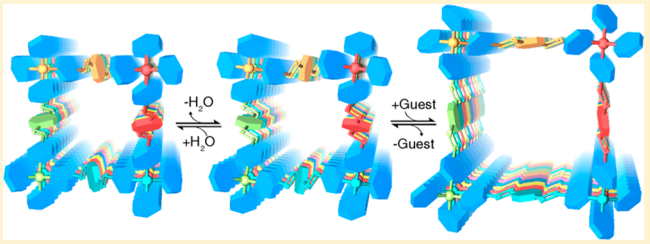

INTRODUCTION

Covalent organic frameworks (COFs) are an emerging class of crystalline, porous materials.[1−3] Although the chemistry for building architecturally robust COFs with permanent porosity is well-developed, very little is known about the dynamics of these frameworks.[4] Preliminary evidence indicating the possibility of dynamics in COF-300, a diamond-net based COF, came from the observation of a step, hysteresis gas adsorption behavior in its isotherm.[5] A second example is the solvent-induced breathing effect observed in LZU-301.[6] Very recently, the molecular weaving COFs enables a new mode of dynamics.[7] In this report, we show how COF-300 is capable of significant contraction and large amplitude expansion when it is subjected to guest inclusions. Synchrotron in-house powder X-ray diffraction (PXRD) analyses with Rietveld refinements were used to determine the crystal structures of each form, and indeed the mechanism for this structural dynamics. Specifically, a significant crystal contraction was observed upon exposure to moisture, and an enormous amount of crystal expansion was found upon inclusion of organic solvents. This resulted in an unit cell volume expansion as large as 50% and an enlargement of the crystallographic channel diameter from 3.3 to 9.6 Å. The switchability of the COF is endowed by the deformation of the tetrahedral nodes, displacement of the interwoven frameworks, and configuration change of the linkers, which enables the different responses to organic vapors and gases varying in sizes/polarity. The *in situ* PXRD of the COF showing the retaining of crystallinity during CO_2 adsorption, indicating the coherent switchability during the structural transformation. With a molecular-level understanding on the adaptive nature of the frameworks, more sophisticated design of dynamic COFs and deliberate control of their dynamics might provide a new dimension in tuning their adsorptive behavior, which are different from those rigid systems requiring strict control of pore sizes/shapes and the chemical environments. The guest-dependent dynamics of COFs would also be a useful feature in pursuing stimuli responsive materials for functional applications.

The challenge to unveil the dynamics of COFs initially arose from the difficulty to prepare highly crystalline, homogeneous, and bulk samples by linking organic building blocks with strong covalent bonds (so-called "crystallization problem"). Recently, COF single crystals suitable for X-ray diffraction have been prepared by slowing down the linkage-formation via imine-exchange strategy, whose procedure remains time-consuming (30−40 days) low-yield (49.8%), and small scale (∼11 mg).[2c] A facile and scalable synthetic protocol is of great importance in tackling the dynamics of COFs through PXRD analysis and property studies towards large-scale functional applications. Therefore, we sought to develop the scalable synthesis of the iconic COF-300, which is known to have a dynamic response, but the underlying factors and mechanism behind that response remains a mystery until now.

Conventionally, microcrystalline COFs were prepared based on using sealed Pyrex tubes (Scheme 1a,c) to provide closed-system for the thermodynamic equilibrium to get crystalline

Received: December 22, 2018

DOI: 10.1021/jacs.8b13691
J. Am. Chem. Soc. XXXX, XXX, XXX−XXX

Scheme 1. Comparison of COF Microcrystal Growth Processes When Using Different Synthetic Protocols

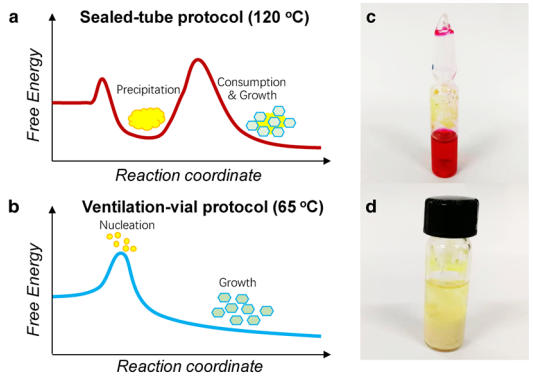

product. However, this method is sensitive, dangerous, and time-intensive, which requires multiple cycles of freeze–pump–thawing for degassing, and calls for the use of a propane/oxygen torch for tube sealing. Due to the freezing or high temperature used in such protocol, amorphous polymers usually participate first, and then the COF crystals grow or convert from them. Consequently, it is difficult to control the morphology of the samples and may lead to multiple phases. In comparison, the ventilation-vial protocol,[8] widely used in MOF chemistry, would ideally be more convenient and efficient, but has yet to be expanded in its practice to COF chemistry (Scheme 1b,d). In the ventilation-vial protocol, it is possible to generate the gradient of acidity or polarity in the system, which provides a homogeneous nucleation process and helps control the morphology of the crystal products. Thus, COF crystals with high crystalline and decent homogeneity can be readily prepared by modulating the crystalized conditions.

RESULTS AND DISCUSSION

Facile and Scareable COF Synthesis. COF-300 was previously synthesized through the acid-catalytic imine-condensation of tetra-(*p*-aminophenyl)-methane (TAM) and terephthalaldehyde (TPA) in 1,4-dioxane sealed in a Pyrex tube and reacted at 120 °C (noted as COF-300-T; Section S1 in Supporting Information, SI), whose products encounter an uncertainty in the interpenetration number.[5] Here, we have developed the ventilation-vial protocol for the facile preparation of COF-300, whose product is noted as COF-300-V (Figure 1). The reaction was successfully performed at temperatures as low as 65 °C with no extra degassing needed. Interestingly, the

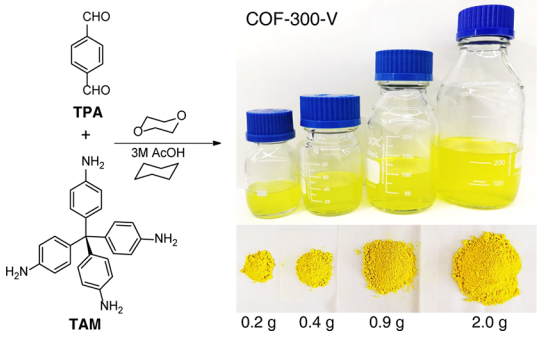

Figure 1. Facile synthesis of COF-300-V using the ventilation protocol easily scale up from 0.2 to 2.0 g of products.

crystallinity and yield of COF-300 can be optimized by modulating the amount of good and poor solvents (i.e., 1,4-dioxane and cyclohexane, respectively; Table S1 in SI). We monitored the solvents before and after the reaction and found that the 1,4-dixoane is vented during the reaction (Table S2 and Figure S1 in SI), which might reduce the solubility and increase the acidity of the system. This ventilation-vial protocol, therefore, may promote the nucleation and accelerate the reaction. The critical components for obtaining such high quality COF crystals are (i) lower temperature to avoid oxidization of aniline groups; (ii) retention of water within the system to sustain reversibility of the imine-condensation reaction; and (iii) reduction of solubility to control the nucleation and crystal growth.[1a]

Notably, this method is easy to scale up to achieve gram-scale samples using (Figure 1) jars with higher yield (up to 90%, Figure S2 and Table S3 in SI) than that of its prior method (only 40% yield). The average laboratory space-time-yields (STY) of COF-300-V was ~1.3 kg/m^3/d, which is comparable with that of the ZIF-8 (~1.3 kg/m^3/d), and higher than that of the MOF-5 (0.21 kg/m^3/d).[9] The Fourier transform infrared (FT-IR, Figure 2a) and the ^{13}C solid-state nuclear magnet resonance

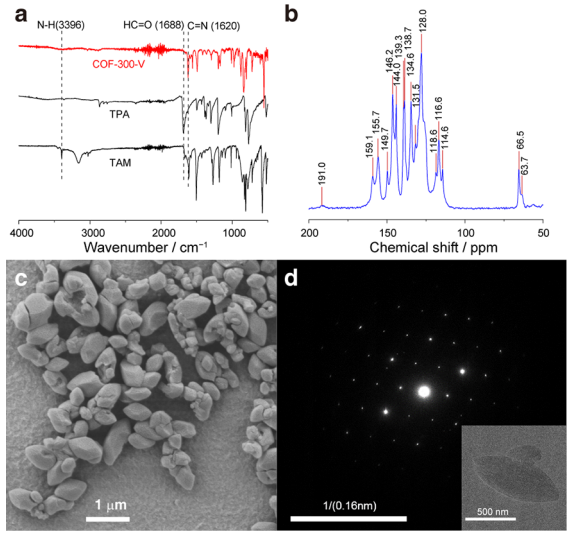

Figure 2. (a) Comparison of FT-IR spectra of COF-300-V with the starting materials, TAM and TPA, showing the formation of the imine-bond with stretching band at 1620 cm^{-1}, and the elimination of the amino (3396 cm^{-1}) and aldehyde groups (1688 cm^{-1}). (b) ^{13}C solid-state NMR of the COF-300-V showing the formation of imine with carbon chemical shift at 159.1 ppm and with only trace residual of aldehyde carbon with chemical shift at 191.0 ppm. (c) SEM image and (d) the SAED pattern with inset of a single crystal showing a homogeneous morphology and single crystallinity in micrometer grain sizes for the obtained COF-300-V.

(NMR, Figure 2b) spectroscopy of the obtained COF-300-V confirmed the formation of imine-bond and the elimination of the starting materials. The scanning electron microscopy (SEM, Figure 2c) and transmission electron microscopy (TEM) with selected-area electron diffraction (SAED, Figure 2d) of COF-300-V showed a homogeneous morphology and single crystallinity of the microsized crystals. Thermogravimetric analyses (TGA) indicate excellent thermal stabilities without decompostion up to 450 °C for both COF-300-H_2O and COF-300-THF samples (Figure S6 in SI).

DOI: 10.1021/jacs.8b13691
J. Am. Chem. Soc. XXXX, XXX, XXX–XXX

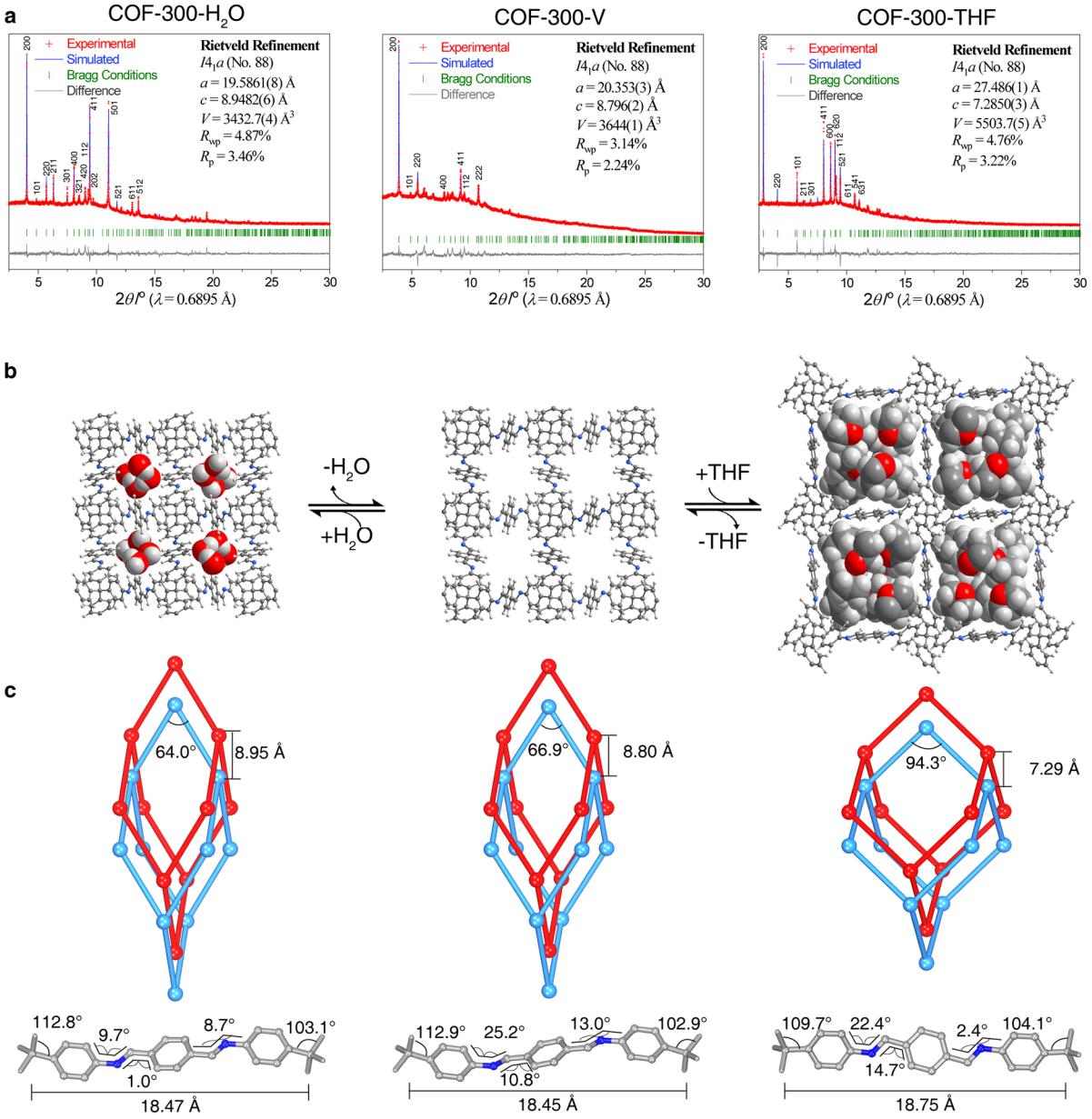

Figure 3. Structural determination of guest-dependent dynamics of COF-300 by the Rietveld refinement of the synchrotron in-house PXRD patterns (a), crystal structures (b), and molecular geometries and configurations (c) of the activated (middle column), hydrated (left column) and THF-solvated (right column) samples of COF-300-V, respectively.

In-house X-ray Diffraction Structural Determination. The crystal structure of activated COF-300-V is determined through synchrotron in-house PXRD analysis (Figure 3, middle column), whose sample was activated in a glass capillary with heating under vacuum. The skeleton of COF-300-V adopts the diamond net with 7-fold interpenetration (**dia**-C7), which is resolved by Rietveld refinement with satisfactory convergence (with R_{wp} = 3.14% and R_p = 2.24%) considering the unit cell parameters [$a = b = 20.353(3)$ Å, $c = 8.796(2)$ Å, $V = 3664(1)$ Å^3], space group ($I4_1a$, No. 88), and atomic coordinates (Section S2 in SI). Noticeably, the PXRD pattern of activated COF-300-V changes when exposed to moisture (relative humidity = ~60% at 298 K) having peak shifts and intensity differences (Figure S10 in the SI). Such water-induced crystal contraction is uncovered with ~6% reduction of the unit cell volume based on the Rietveld refinement (Figure 3, left column). Interestingly, water molecules formed hydrogen bonding chains in the channels and the framework adapts to these chains and turned into a contracted form.

Remarkably, the COF-300-V represents a large amplitude crystal expansion upon inclusion of organic solvents. Giant crystal expansion is observed in its solvated phase after inclusion of tetrahydrofuran (THF) resulting in ~50% increment of the crystallographic cell volume (Figure 3, right column; space group: $I4_1a$; $a = b = 27.486(1)$ Å, $c = 7.285(3)$ Å, $V = 5503.7(5)$ Å^3; R_{wp} = 4.76% and R_p = 3.22%). Comparing the crystal structures of contracted and expanded COF-300-V, the channel sizes are enlarged in 3-folds (from 3.3 to 9.6 Å), and their pore volumes are increase for 4.6 times (from 0.17 to 0.78 cm^3/g estimated by the PLATON), respectively.

As shown in Figure 3c, the mechanism of the dynamics of the COF-300-V is attributed to the deformation of the node geometry, displacement between frameworks, and the configuration change of the organic linkers having various bond angles,

DOI: 10.1021/jacs.8b13691
J. Am. Chem. Soc. XXXX, XXX, XXX−XXX

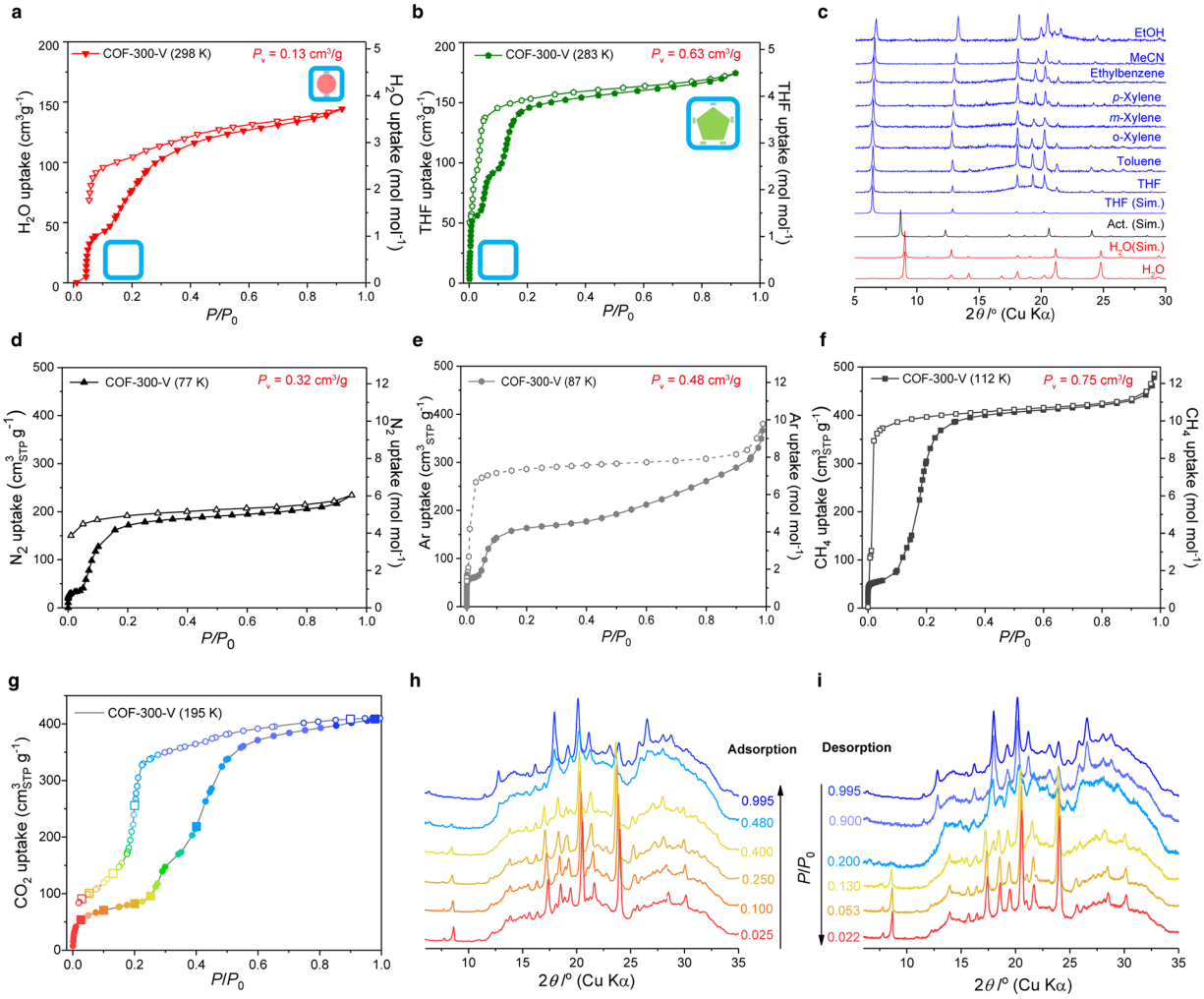

Figure 4. (a) THF vapor adsorption isotherm at 283 K. (b) Water adsorption isotherm at 298 K. (c) PXRD patterns of COF-300-V upon inclusions of organic solvents and water. (d) N_2 adsorption isotherm at 77 K. (e) Ar adsorption isotherm at 87 K. (f) CH_4 adsorption isotherm at 112 K. (g) CO_2 adsorption isotherm at 195 K and the *in situ* PXRD patterns at representative equilibrium pressures for the adsorption (h) and desorption branch (i), respectively (the colors represent different status of the structural transformation: red, lattice unchanged; yellow to green, lattice gradually change; blue, expanded phase).

torsion angles and node distances. It is obvious that the node geometry varied from 64.0° to 94.3° is the most significant change adapting to the included guests. Such contraction-expansion-contraction transformation is reversiable at ambient conditon upon the solvantion and desolvation of THF (Figures S12 and S13 in SI). The structural transformation is also evident by the ^{13}C solid state NMR spectra of COF-300-H_2O and COF-300-THF having changes in chemical shifts (Figure S8 in SI). The host−guest interaction and guest−guest interaction are known as the driving force to make such changes.[10]

Guest-dependent Responses for Adsorption. The guest-dependent dynamics of COF-300 can be visualized by adsorption isotherms using various vapors as probes. As shown in Figure 4a, COF-300 can capture water easily at low relative pressure having a steep uptake at ~0.05, followed by a shallow step with triple uptake capacity reaching four water molecules per mole. This is consistent with the crystal structure of the COF-300-H_2O to have a smaller pore volume of 0.13 cm^3/g. As shown in Figure 4b, the THF uptake of COF-300 exhibits three steps of steep uptake. This shows the inclusion of the THF triggers the crystal expansion to have a larger pore volume of 0.63 m^3/g. Such behavior is also consistent with other vapor adsorption isotherms of 1,4-dixoane and cyclohexane (Figures S15 and S16 in SI). PXRD patterns of the solvated phases of COF-300 also support the crystal expansion in other organic solvents (Figure 4c).

The sorption isotherms using various gases as probes also reveal different degrees of crystal expansion at each critical temperatures (Section S3 in the SI). As shown in Figure 4d, the N_2 adsorption isotherms at 77 K exhibits a small steep step followed by a shallow step with lower uptake to have a smaller pore volume of 0.32 cm^3/g. The Ar adsorption isotherm at 87 K displays a higher uptake for the first step followed by a shallow step to realize a larger pore volume of 0.48 cm^3/g. Finally, the CH_4 adsorption isotherm at 112 K shows a steep uptake at lower relative pressure followed by a significant step to have the largest pore volume of 0.75 cm^3/g. It is worth noting that the dynamic behavior is sensitive to the sample quality (Figures S14 and S19 in SI). The adsorption isotherms of COF-300-V is more reproducible than those of the COF-300-T (Figures S20 and S21 in SI).

Coherent Switchability of Structural Transformation. For the first time in COF chemistry, the gas-responsive structural transformation is directly observed here through *in*

DOI: 10.1021/jacs.8b13691
J. Am. Chem. Soc. XXXX, XXX, XXX−XXX

situ PXRD analysis (Section S4 in SI) during CO_2 adsorption at 195 K. As shown in Figure 4g, stepwise and hysteresis CO_2 adsorption isotherms of COF-300-V were reproducible using both gas sorption analyzer (Figure S) and in-situ apparatus, which can be qualitatively classified based on the *in situ* PXRD patterns of COF-300-V for each uptake at the equilibrium pressures (Figure 4h,i, Figures S22 and S23 in SI): (i) Lattice constant of COF-300-V remains unchanged from vacuum to $P/P_0 = 0.05$ having a steep CO_2 uptake characteristic of micropores with relative strong framework−CO_2 interactions; (ii) Only slight lattice expansion is observed from $P/P_0 = 0.05-0.4$, during which a second-step uptake occurred after a gradual increment suggesting a rearrangement of adsorbates; (iii) A significant lattice expansion happens when the P/P_0 is greater than 0.48. Such gas-induced structural transformation is generally reversible during the desorption process but with hysteresis at lower P/P_0. The lattice shrinks suddenly at $P/P_0 \sim 0.13$ when a large amount of CO_2 is extracted out from the pores. It is worth noting that the coherent switchability during the structural transformation might be attributed to the highly interpenetrated nature of the COF, which represents a domino effect for simultaneous geometric changes.

CONCLUSION

By controlling the nucleation and crystal growth, the iconic COF-300 has been prepared with high crystallinity and homogeneity through a facile and scalable ventilation-vial protocol. We uncovered the guest-dependent dynamics in COFs for the first time using various probes. With its exceptional adaptability and coherent switchability, this 3D dynamic COF represents a versatile platform for studying the structural dynamics at a molecular level in relation to external stimuli. Furthermore, with this fundamental understanding of the mechanism of structural dynamics, the switchability and the response to a specific guest could therefore be manipulated, in the future, for realizing functional applications.[11]

EXPERIMENTAL SECTION

Materials. TAM was synthesized and purified according to the literature procedure.[12] Other starting materials are purchased from commercial sources.

Synthesis of COF-300-V. A mixture of TPA (12 mg, 0.089 mmol) and TAM (20 mg, 0.052 mmol) was dissolved in 1.6 mL of anhydrous 1,4-dioxane and 0.4 mL cyclohexane within a 4 mL vial under sonication. Then 0.4 mL of aqueous acetic acid (3 mol/L) was added into the vial, which was capped and put into an oven at 65 °C for 72 h. The yellow fine powder was COF-300-V isolated by hot filtration, and washed with 1,4-dioxane and THF, which was evacuate and heated at 120 °C to give COF-300-V (15 mg, 58.4% yield based on TPA). Elemental Analysis: Calcd. for $C_{41}H_{28}N_4 \cdot (H_2O)_2$: C, 80.37; H, 5.26; N, 9.14%. Found: C, 79.02; H, 5.50; N, 9.40%.

Scale-Up Synthesis of COF-300-V. A mixture of TPA (1.24 g, 9.20 mmol) and TAM (2.07 g, 5.37 mmol) was dissolved in 192 mL of anhydrous 1,4-dioxane and 48 mL cyclohexane within a 500 mL bottle under sonication. Then 48 mL of aqueous acetic acid (3 mol/L) was added into the bottle slowly, which was capped and put into an oven at 65 °C for 72 h. The yellow fine powder was isolated by hot filtration, and washed with dioxane and THF several times, which was evacuated and heated at 120 °C to give COF-300-V (2.0 g, 75% yield based on TPA).

Characterization. The FT-IR spectra were recorded on neat samples in the range of 4000−500 cm^{-1} on a PerkinElmer FT-IR Spectrometer equipped with single reflection diamond ATR module. ^1H NMR spectroscopy were recorded on AVANCE III HD 500 MHz spectrometer. The solid-state ^{13}C NMR spectra were recorded on an Agilent DD2 600 MHz NMR spectrometer with cross-polarization magic angle-spinning (CP/MAS). The scanning electron microscopy images were collected on the on JSM-7800F PRIME extreme resolution field emission SEM. The TEM image is collected on a 120 kV JEOL JEM-1400plus microscope. The elemental analyses were performed on Perkinelmer SERIES ll 2400 (Clarus 580). TGA were performed at a rate of 5 °C min^{-1} under N_2 with NETZSCH TG-209.

Gas Adsorption. The as-synthesized sample was exchanged with 1,4-dioxane for at least 5 times until the solvent was color-less, then transferred to a Soxhlet extractor and extracted with 1,4-dioxane for 3 days, THF for 1 day respectively. The fully exchanged sample was then degassed at 120 °C for 10 h before gas adsorption measurement. Low-pressure gas adsorption isotherms were measured volumetrically using a Quantachrome iQ (N_2 and CH_4) or MicrotacBELsorp Max (CO_2) gas sorption analyzer. A liquid nitrogen bath was used for the temperatures controlled at 77 and 112 K (with a CryoSyncTM from Quantachrome); a dry ice-methanol bath was used for the temperature controlled at 195 K. Stainless steel recirculating Dewar connected to a Julabo F25-ME isothermal bath filled with ethylene glycol aqueous solution (1:3, *v*/*v*), for which the temperature stability is ±0.02 °C, was used for temperatures controlled at 273, 283, and 298 K. The organic vapor and H_2O adsorption isotherms were collected using Micro-tracBELSorp-Aqua^3 adsorption apparatus with a water circulator bath as mentioned above. Ultrahigh grade of gases (99.999%) such as He, N_2, CH_4 and CO_2 were used through all the experiments. Anhydrous solvents (i.e., THF, 1,4-dioxane, and cyclohexane) and ultrapure water were used for vapor adsorption, which were degassed with at least five freeze−pump−thaw cycles before isotherms collection.

X-ray Diffraction Analyses. PXRD patterns were recorded on Bruker D8 Advance diffractometer with Cu Kα radiation with the voltage of 40 kV. Data were collected in the 2θ range of 5−30° with the steps of 0.02°. The hydrated sample was haddled in air at room temperature and paved on a rotation silicon sample stage. The solvated samples such as COF-300-THF were dropwisely added with solvents to the sample stage and covered with Kapton film. Specially, diffraction data for Rietveld refinements were collected in the beamline BL14B1 at Shanghai Synchrotron Radiation Facility with the capillary transmission mode. The rigirously guest-free sample of COF-300-V was sealed under high vacuum after heating at 120 °C in a glass capillary. The sample of COF-300-THF was sealed under saturated THF vapor to avoid guest escape. The sample of COF-300-H_2O was sealed at ambient condition under 60% humidity. The refined crystal structures have been deposited in the Cambridge Structural Database (CCDC #1887488-1887490).

ASSOCIATED CONTENT

Supporting Information

The Supporting Information is available free of charge on the ACS Publications website at DOI: 10.1021/jacs.8b13691.

Syntheses andcharacterization, PXRD analyses, adsorption isotherms and *in situ* PXRD patterns (PDF)
Crystal structure of COF-300-V (CIF)
Crystal Structure of COF-300-THF (CIF)
Crystal Structure of COF-300-H_2O (CIF)

AUTHOR INFORMATION

Corresponding Authors

*zhouhl@shanghaitech.edu.cn
*zhangyb@shanghaitech.edu.cn

ORCID

Hao-Long Zhou: 0000-0002-5007-6535
Yue-Biao Zhang: 0000-0002-8270-1067

Author Contributions

†These author contributed equally.

Notes

The authors declare no competing financial interest.

DOI: 10.1021/jacs.8b13691
J. Am. Chem. Soc. XXXX, XXX, XXX−XXX

■ ACKNOWLEDGMENTS

This work is supported by the National Natural Science Foundation of China (No. 21522105 and 51861145313). H.-L.Z. is financially supported by the National Postdoctoral Program for Innovative Talents (BX201700272). The SEM and TEM characterization are supported by CħEM (Prof. O. Terasaki, grant #EM02161943), and the XRD (Dr. N. Yu) and gas adsorption (Ms. L. Long) measurements are supported by the SPST Analytical Center at ShanghaiTech University. The authors thank beamline BL14B1 at Shanghai Synchrotron Radiation Facility for providing the beam time and assistance during experiments, Dr. J. Sonoda from MicrotracBEL Corp. for coordinating the *in situ* XRD measurement, Prof. W. Wang and Dr. S.-Y. Ding at Lanzhou University for discussion of NMR spectroscopy, and Mr. K. E. Cordova at the Berkeley Global Science Institute for beneficial discussions.

■ REFERENCES

(1) (a) Côté, A. P.; Benin, A. I.; Ockwig, N. W.; O'Keeffe, M.; Matzger, A. J.; Yaghi, O. M. Porous, Crystalline, Covalent Organic Frameworks. *Science* **2005**, *310*, 1166. (b) El-Kaderi, H. M.; Hunt, J. R.; Mendoza-Cortés, J. L.; Côté, A. P.; Taylor, R. E.; O'Keeffe, M.; Yaghi, O. M. Designed Synthesis of 3D Covalent Organic Frameworks. *Science* **2007**, *316*, 268. (c) Diercks, C.; Yaghi, O. M. The Atom, the Molecule, and the Covalent Organic Framework. *Science* **2017**, *355*, eaal1585.

(2) (a) Ascherl, L.; Sick, T.; Margraf, J. T.; Lapidus, S. H.; Calik, M.; Hettstedt, C.; Karaghiosoff, K.; Döblinger, M.; Clark, T.; Chapman, K. W.; Auras, F.; Bein, T. Molecular Docking Sites Designed for the Generation of Highly Crystalline Covalent Organic Frameworks. *Nat. Chem.* **2016**, *8*, 310. (b) Jin, E.; Asada, M.; Xu, Q.; Dalapati, S.; Addicoat, M. A.; Brady, M. A.; Xu, H.; Nakamura, T.; Heine, T.; Chen, Q.; Jiang, D. Two-Dimensional sp^2 Carbon−Conjugated Covalent Organic Frameworks. *Science* **2017**, *357*, 673. (c) Ma, T.; Kapustin, E. A.; Yin, S. X.; Liang, L.; Zhou, Z.; Niu, J.; Li, L.; Wang, Y.; Su, J.; Li, J.; Wang, X.; Wang, W. D.; Wang, W.; Sun, J.; Yaghi, O. M. Single-Crystal X-ray Diffraction Structures of Covalent Organic Frameworks. *Science* **2018**, *361*, 48. (d) Evans, A. M.; Parent, L. R.; Flanders, N. C.; Bisbey, R. P.; Vitaku, E.; Kirschner, M. S.; Schaller, R. D.; Chen, L. X.; Gianneschi, N. C.; Dichtel, W. R. Seeded Growth of Single-Crystal Two-Dimensional Covalent Organic Frameworks. *Science* **2018**, *361*, 52.

(3) (a) Doonan, C. J.; Tranchemontagne, D. J.; Glover, T. G.; Hunt, J. R.; Yaghi, O. M. Exceptional Ammonia Uptake by a Covalent Organic Framework. *Nat. Chem.* **2010**, *2*, 235. (b) Lin, S.; Diercks, C. S.; Zhang, Y.-B.; Kornienko, N.; Nichols, E. M.; Zhao, Y.; Paris, A. R.; Kim, D.; Yang, P.; Yaghi, O. M.; Chang, C. J. Covalent Organic Frameworks Comprising Cobalt Porphyrins for Catalytic CO_2 Reduction in Water. *Science* **2015**, *349*, 1208. (c) Fang, Q.; Wang, J.; Gu, S.; Kaspar, R. B.; Zhuang, Z.; Zheng, J.; Guo, H.; Qiu, S.; Yan, Y. 3D Porous Crystalline Polyimide Covalent Organic Frameworks for Drug Delivery. *J. Am. Chem. Soc.* **2015**, *137*, 8352. (d) Sun, Q.; Aguila, B.; Perman, J.; Earl, L.; Abney, C.; Cheng, Y.; Wei, H.; Nguyen, N.; Wojtas, L.; Ma, S. Postsynthetically Modified Covalent Organic Frameworks for Efficient and Effective Mercury Removal. *J. Am. Chem. Soc.* **2017**, *139*, 2786. (e) Lin, G.; Ding, H.; Yuan, D.; Wang, B.; Wang, C. A Pyrene-Based, Fluorescent Three-Dimensional Covalent Organic Framework. *J. Am. Chem. Soc.* **2016**, *138*, 3302. (f) Wang, S.; Wang, Q.; Shao, P.; Han, Y.; Gao, X.; Ma, L.; Yuan, S.; Ma, X.; Zhou, J.; Feng, X.; Wang, B. Exfoliation of Covalent Organic Frameworks into Few-Layer Redox-Active Nanosheets as Cathode Materials for Lithium-Ion Batteries. *J. Am. Chem. Soc.* **2017**, *139*, 4258. (g) Dey, K.; Pal, M.; Rout, K. C.; Kunjattu, S.; Das, A.; Mukherjee, R.; Kharul, J. K.; Banerjee, R. Selective Molecular Separation by Interfacially Crystallized Covalent Organic Framework Thin Films. *J. Am. Chem. Soc.* **2017**, *139*, 13083. (h) Han, X.; Huang, J.; Yuan, C.; Liu, Y.; Cui, Y. Chiral 3D Covalent Organic Frameworks for High Performance Liquid Chromatographic Enantioseparation. *J. Am. Chem. Soc.* **2018**, *140*, 892. (i) Zhang, G.; Tsujimoto, M.; Packwood, D.; Duong, N. T.; Nishiyama, Y.; Kadota, K.; Kitagawa, S.; Horike, S. Construction of a Hierarchical Architecture of Covalent Organic Frameworks via a Postsynthetic Approach. *J. Am. Chem. Soc.* **2018**, *140*, 2602.

(4) (a) Horike, S.; Shimomura, S.; Kitagawa, S. Soft Porous Crystals. *Nat. Chem.* **2009**, *1*, 695. (b) Férey, G.; Serre, C. Large Breathing Effects in Three-Dimensional Porous Hybrid Matter: Facts, Analyses, Rules and Consequences. *Chem. Soc. Rev.* **2009**, *38*, 1380. (c) Schneemann, A.; Bon, V.; Schwedler, I.; Senkovska, I.; Kaskel, S.; Fischer, R. A. Flexible Metal−Organic Frameworks. *Chem. Soc. Rev.* **2014**, *43*, 6062. (d) Zhang, J.-P.; Liao, P.-Q.; Zhou, H.-L.; Lin, R.-B.; Chen, X.-M. Single-Crystal X-ray Diffraction Studies on Structural Transformations of Porous Coordination Polymers. *Chem. Soc. Rev.* **2014**, *43*, 5789.

(5) (a) Uribe-Romo, F. J.; Hunt, J. R.; Furukawa, H.; Klock, C.; O'Keeffe, M.; Yaghi, O. M. A Crystalline Imine-Linked 3-D Porous Covalent Organic Framework. *J. Am. Chem. Soc.* **2009**, *131*, 4570. (b) Ma, T.; Li, J.; Niu, J.; Zhang, L.; Etman, A. S.; Lin, C.; Shi, D.; Chen, P.; Li, L.-H.; Du, X.; Sun, J.; Wang, W. Observation of Interpenetration Isomerism in Covalent Organic Frameworks. *J. Am. Chem. Soc.* **2018**, *140*, 6763.

(6) (a) Zhang, Y.-B.; Su, J.; Furukawa, H.; Yun, Y.; Gándara, F.; Duong, A.; Zou, X.; Yaghi, O. M. Single-Crystal Structure of a Covalent Organic Framework. *J. Am. Chem. Soc.* **2013**, *135*, 16336. (b) Ma, Y.-X.; Li, Z.-J.; Wei, L.; Ding, S.-Y.; Zhang, Y.-B.; Wang, W. A Dynamic Three-Dimensional Covalent Organic Framework. *J. Am. Chem. Soc.* **2017**, *139*, 4995.

(7) (a) Liu, Y.; Ma, Y.; Zhao, Y.; Sun, X.; Gándara, F.; Furukawa, H.; Liu, Z.; Zhu, H.; Zhu, C.; Suenaga, K.; Oleynikov, P.; Alshammari, A. S.; Zhang, X.; Terasaki, O.; Yaghi, O. M. Weaving of Organic Threads into a Crystalline Covalent Organic Framework. *Science* **2016**, *351*, 365. (b) Liu, Y.; Ma, Y.; Yang, J.; Diercks, C. S.; Tamura, N.; Jin, F.; Yaghi, O. M. Molecular Weaving of Covalent Organic Frameworks for Adaptive Guest Inclusion. *J. Am. Chem. Soc.* **2018**, *140*, 16015.

(8) Eddaoudi, M.; Kim, J.; Rosi, N. L.; Vodak, D. T.; Wachter, J.; O'Keeffe, M.; Yaghi, O. M. Systematic Design of Pore Size and Functionality in Isoreticular MOFs and Their Application in Methane Storage. *Science* **2002**, *295*, 469.

(9) Yilmaz, B.; Trukhan, N.; Müller, U. Industrial Outlook on Zeolites and Metal Organic Frameworks. *Chin. J. Catal.* **2012**, *33*, 3.

(10) Serre, C.; Mellot-Draznieks, C. M.; Surblé, S.; Audebrand, N.; Filinchuk, Y.; Férey, G. Role of Solvent-Host Interactions That Lead to Very Large Swelling of Hybrid Frameworks. *Science* **2007**, *315*, 1828.

(11) (a) Colombo, V.; Montoro, C.; Maspero, A.; Palmisano, G.; Masciocchi, N.; Galli, S.; Barea, E.; Navarro, J. A. R. Tuning the Adsorption Properties of Isoreticular Pyrazolate-Based Metal−Organic Frameworks through Ligand Modification. *J. Am. Chem. Soc.* **2012**, *134*, 12830. (b) Serra-Crespo, P.; Berger, R.; Yang, W.; Gascon, J.; Kapteijn, F. Separation of CO_2/CH_4 Mixtures Over NH_2-MIL-53−An Experimental and Modelling Study. *Chem. Eng. Sci.* **2015**, *124*, 96. (c) Li, L.; Lin, R.-B.; Krishna, R.; Wang, X.; Li, B.; Wu, H.; Li, J.; Zhou, W.; Chen, B.-L. Flexible-Robust Metal-Organic Framework for Efficient Removal of Propyne from Propylene. *J. Am. Chem. Soc.* **2017**, *139*, 7733. (d) Zhang, J.-P.; Zhou, H.-L.; Zhou, D.-D.; Liao, P.-Q.; Chen, X.-M. Controlling Flexibility of Metal−Organic Frameworks. *Natl. Sci. Rev.* **2018**, *5*, 907.

(12) Plietzsch, O.; Schilling, C. I.; Tolev, M.; Nieger, M.; Richert, C.; Muller, T.; Bräse, S. Four-Fold Click Reactions: Generation of Tetrahedral Methane- and Adamantane-Based Building Blocks for Higher-Order Molecular Assemblies. *Org. Biomol. Chem.* **2009**, *7*, 4734.

DOI: 10.1021/jacs.8b13691
J. Am. Chem. Soc. XXXX, XXX, XXX−XXX